Department of Pesticide Regulation

Brian R. Leahy
Director

M E M O R A N D U M

Edmund G. Brown Jr.
Governor

TO: Randy Segawa
Environmental Program Manager I
Environmental Monitoring Branch

FROM: Frank Spurlock, Ph.D *Original signed by*
Research Scientist III
Environmental Monitoring Branch
916-324-4124

Bruce Johnson, Ph.D *Original signed by*
Research Scientist III
Environmental Monitoring Branch

Atac Tuli, Ph.D. *Original signed by*
Environmental Scientist
Environmental Monitoring Branch

DATE: February 8, 2013

SUBJECT: HYDRUS SIMULATION OF CHLOROPICRIN AND 1,3-DICHLOROPROPENE TRANSPORT AND VOLATILIZATION IN THE LOST HILLS FUMIGATION TRIALS

ABSTRACT
We compared HYDRUS 2D/3D simulated fluxes to flux estimates based on Industrial Source Short Term (ISC) inverse-modeling (i.e. back-calculation) of fumigant air concentrations from a study in Lost Hills, California (Ajwa and Sullivan, 2012). Lost Hills field 1 data were used to calibrate the HYDRUS model. Subsequent HYDRUS simulations of field 2 and field 3 chloropicrin and 1,3-dichloropropene (1,3-D) flux were conducted using the calibrated HYDRUS model without further adjustment. HYDRUS accurately described fumigant soil-gas concentrations, soil-temperature and water content, and both pre- and post-tarpcut fumigant volatilization throughout the field 1 study period. The calibration results show that the model was adequately representing basic process of heat transport, fumigant partitioning, fumigant degradation and volatilization. HYDRUS-simulated cumulative and discrete peak fluxes for fields 2 and 3 were within the likely range of uncertainty of the ISC estimates. However, in all fields HYDRUS tended to predict the occurrence of peak fumigant fluxes one to two days later than in the ISC estimates.

INTRODUCTION
This memorandum summarizes HYDRUS 2D/3D modeling of the June 2011 Lost Hills field fumigation study. That study investigated broadcast application of chloropicrin/1,3-D to 3 fields under a “totally impermeable film” (TIF). Ajwa and Sullivan (2012) provided ISC inverse-modeled (“back calculated”) chloropicrin and 1,3-D flux estimates for all three fields. Extensive

soil sampling and site characterization data were collected by DPR (Tuli, 2011), and U.S. Department of Agriculture-Agricultural Research Service (USDA-ARS) measured fumigant soil gas concentrations (Gao et al., 2013). HYDRUS modeling was conducted with those data using a conventional "calibration/validation" type procedure, where fumigant flux and soil-gas concentration data from one field were used to calibrate HYDRUS, and fluxes from the remaining two fields then simulated with all model input variables independently estimated, measured, or obtained from the initial calibration.

Although a calibration/validation approach to modeling was used here, the results do not represent a true model "validation" in the conventional sense. Typically models are "validated" against measured data. Fumigant fluxes are not usually measured directly in the field in the same sense that air concentrations, for example, are direct field measurements. Instead fumigant fluxes are typically modeled from measured air concentrations using vertical profile methods (e.g., the aerodynamic method, AD; Parmele et al., 1972; Majewski, 1996) or inverse modeling with an atmospheric dispersion model such as the U.S. Environmental Protection Agency Industrial Source Complex Short Term model (ISC; Ross et al., 1996; Sullivan et al., 2004; Johnson et al., 2010). Discrete period-mean flux estimates based on measured time-weighted average fumigant air concentrations have a relatively high level of uncertainty. Majewski (1996) estimated a mean error of ~ 50% for discrete fluxes obtained using the AD method. Uncertainty in inverse modeled fluxes has not been quantified, but is known to be substantial (Johnson and Spurlock, 2013; Sullivan et al., 2004; Wang et al., 2006; Sax and Isakov, 2003). Inverse modeling using ISC is generally assumed to yield flux predictions within a factor of 2 of actual flux (Hsieh et al., 1995; Ross et al., 1996). In this study HYDRUS is calibrated, and subsequently compared, to ISC inverse-modeled cumulative and discrete flux estimates. Those estimates have substantial but unknown error. Consequently the HYDRUS evaluation here is best considered as a comparison of two flux estimation procedures, as opposed to a conventional model validation. Below we summarize the Lost Hills study, data collected, HYDRUS calibration and subsequent comparison to the inverse-modeled and measured field data.

LOST HILLS DATA COLLECTION AND MODELING

Study overview and objectives

The objectives for the Lost Hills study were to:

1. Determine emission ratios and period mean flux densities for chloropicrin and 1,3-D under a 30 cm deep broadcast application covered by a TIF
2. Determine maximum post-tarpcut period mean flux densities as a function of tarp holding time (time from application to tarp cut)
3. Collect comprehensive flux, subtarp gas concentration, soil and site data for use in comparing ISC inverse-modeled and HYDRUS simulated fumigant flux

On June 4, 2011, simultaneous 30 cm deep broadcast shank applications of Pic-Chlor 60 (EPA Reg. No. 8536-8) were made to three fields using a Nobel plow (Table 1). The minimum field separation was 250 m to avoid confounding of air-samples among fields. The fields were prepared in accordance with label requirements specifying good agricultural practices for pre-application tillage and soil moisture requirements, and each covered with a Raven VaporSafe^{TM} TIF tarp.

Field 1 data were used for HYDRUS calibration, and field 2 and 3 fluxes then simulated with field 1 calibrated inputs and site-specific soil data. HYDRUS simulated field 2 and 3 discrete period mean flux densities and cumulative fluxes were compared to inverse-modeled fluxes estimated using the dispersion model ISC.

Table 1. Summary of Field 1-3 Fumigant Applications.

Field number	Acres	Chloropicrin/1,3-D rate (lbs/acre)	Tarp-holding time (d)[A]	USDA soil type
1	8.16	341/231	16	Milham Sandy Loam (92%), Kimberlina Fine Sandy Loam (8%)
2	1.97	326/221	10	Milham Sandy Loam (100%)
3	2.03	354/240	5	Milham Sandy Loam (100%)

[A] Time between application and tarp-cut. Flux data were collected for 2 days after tarpcut in each field.

Field data collected

Soil sampling

Undisturbed soil cores were collected in field 1 from nine locations, and four locations in both fields 2 and 3 prior to application. At each location a single core sample was collected to a depth of 80 cm in 20 cm increments. Thus, a total of 68 core samples were collected from all three fields. Bulk density and initial soil-water content were determined for each soil core segment. Disturbed soil samples were collected at each location and depth of the undisturbed core segments, and soil texture and organic carbon content (OC) were determined on these samples. Finally, four 80 cm x 20 cm increment cores were collected from the surrogate plot adjacent to field 1 to estimate field 1 end-of-study water content.

Surrogate plot

A surrogate plot (Figure 1) was installed adjacent to field 1. The surrogate plot was prepared identically to the three fields and covered with TIF tarp using a fumigation application rig, but with no actual application of fumigant. The surrogate plot was used for measuring under-tarp soil temperature data for modeling (Figure A-1, Appendix). relative humidity (Figure A-2, Appendix) and barometric pressure data (Figure A-3, Appendix) were also collected for later

diagnostic purposes if needed. Probe locations in the surrogate plot for replicate measurement of surface (undertarp) relative humidity (RH), undertarp temperature in the air-gap between the soil and the tarp, and both temperature and soil-water content at 10, 30, 50 and 70 cm depths are shown in Figure 1. Data were collected every five minutes.

Soil-gas sampling

Soil gas sampling probes were placed in field 1 immediately after application. Field 1 fumigant soil gas concentrations measured between the tarp and soil surface were used in HYDRUS calibration (N = 24 each sampling time). The calibrated model gas concentration predictions were then compared to soil gas concentrations measured at 25, 45, 70 and 100 cm depths (n = 12 each sampling time). The undertarp and soil gas data were collected at 1.4, 2.4, 3.4, 6.4, 9.4, 12.4, 15.4 and 18.4 days. Soil gas sampling was performed using the method described in Qin et al. (2011).

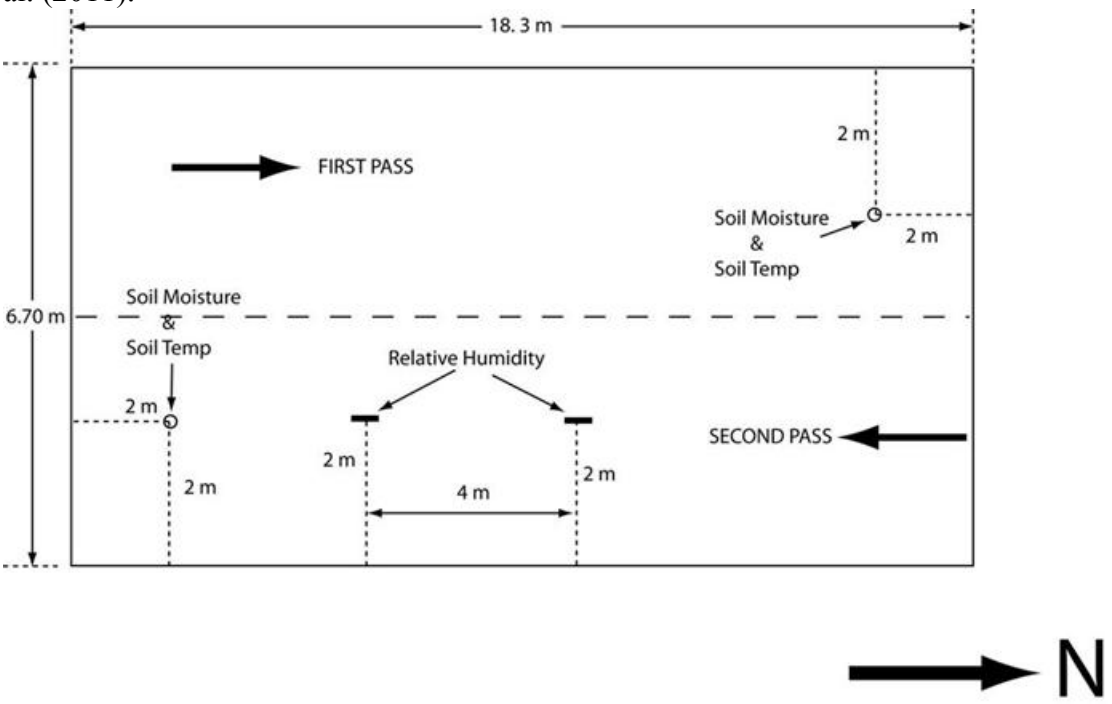

Figure 1. Layout and dimensions of surrogate plot adjacent to field 1.

Fumigant flux data

For each field, off-site time-averaged chloropicrin and 1,3-D air concentrations at 1.5 m height were collected (n=16, field 1; n=8, fields 2 and 3) for six hour periods in the first two days after application, followed by 12 hour periods until tarp-cut, and 6 hour periods for an additional 2 days following tarp-cut. The ISC inverse-modeling procedure to estimate flux is detailed in Ajwa and Sullivan (2012). Most of the flux data reported by Ajwa and Sullivan (2012) were directly used in the HYDRUS field 1 calibration and subsequent comparison to field 2 and 3 results.

However, flux calculation errors for a few periods were discovered in the original data submission and corrected. This, in conjunction with minor differences in DPR's data analysis methods, resulted in slightly different flux data used for the HYDRUS evaluation here as compared to the original submission (Ajwa and Sullivan, 2012).

Preliminary Data Analysis

Soil analysis

Soil-water retention was experimentally determined for each core segment at 0.052, 0.1, 0.33 and 0.8 bars tension. Saturated water content was determined from soil bulk density using an assumed particle density of 2.65 g cm^{-3}. Average soil-water hydraulic parameters for each field (Appendix Table A-1) were determined by fitting the average retention water content data to the van Genuchten model (van Genuchten, 1980) using RETC (van Genuchten et al., 1991) and an assumed residual soil-water content of 0.039 (average for sandy loam soils, Carsel and Parrish, 1988). In each field, soil-organic carbon was determined using mass loss on ignition data reported by the University of California Division of Agricultural and Soil Resources Laboratory data (Ajwa and Sullivan, 2012) and dichromate reduction data determined by DPR (Table A-1, Appendix 1).

Edge effects on flux and off-site air concentrations

While Ajwa and Sullivan (2012) provided Lost Hills whole field flux estimates based on ISC inverse modeling, Gao et al. (2013) measured fumigant fluxes at specific field 1 locations using 50 cm long dynamic flux chambers (DFC). DFC measurement locations included a bare ground strip at 0 to 50cm from the edge of tarp, and a second set of measurements 2 m from the tarp edge. DFC volatilization fluxes at the 2 m distance were essentially negligible (<0.5 ug m^{-2} s^{-1}, with most values <0.05 ug m^{-2} s^{-1}; Gao et al., 2013), but mean fluxes measured at the 0-50 cm distance from the tarp edge were > 100 ug m^{-2} s^{-1} over the first two days. Depending on how far these flux rates extend beyond the edge of the tarp, there is a potential for confounding measured off-site air concentrations, and therefore the inverse-modeled flux estimates. Any potential effect is expected to be greatest for tarps with extremely low permeabilities (such as TIF). To investigate this question we conducted a preliminary HYDRUS simulation to assess relative flux as a function of distance from the tarp edge under field 1 conditions.

The edge-of-field HYDRUS simulations relied on high diffusion assumptions of dry soil (uniform $\theta = 0.13$), and an initial fumigant soil distribution spread uniformly at the 30 cm depth to tarp edge. The assumptions were intended to assess worst-case potential field border flux contribution. The HYDRUS simulations showed a very rapid decline in volatilization flux with distance from the tarp edge (Figure 2), consistent with reported exponential declines in 0.45 m depth soil fumigant gas concentrations with lateral distance from tarp edges (Wang et al., 2010). The simulations yielded a total border contribution of 2% (8 acre, field 1) and 4% (2 acre, fields 2 and 3) of the total 7 d end of simulation emission ratio of 0.07. Although the simulated

cumulative flux is low, these potential contributions do add some additional uncertainty to the inverse-modeled ISC flux estimates.

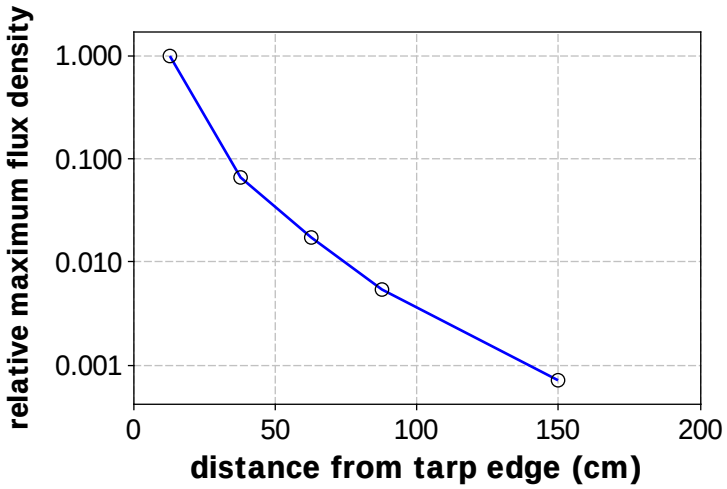

Figure 2. Relative maximum flux density with distance from edge of tarp determined in preliminary HYDRUS simulations to evaluate potential edge effects. Relative maximum 6 hour flux densities were simulated for 0-25, 25-50, 50-75, 75 – 100 and 100 – 200 cm from edge of a TIF tarped 6000 cm wide domain.

Model Calibration

Input variables

In addition to application rate, initial fumigant distribution, and model domain geometry, several input variables are required to execute the HYDRUS model (Table A-2, Appendix). Prior to the Lost Hills study, a sensitivity analysis was performed to guide field sampling design and subsequent modeling (Spurlock et al., 2012). Based on that analysis, input variables with the greatest influence on simulated flux *and* that cannot be accurately measured or estimated in the field are the boundary layer depth (*d*, cm, a measure of tarp permeability), degradation rate (k_1,d^{-1}) and soil sorption coefficient (K_{OC}, ml g^{-1}). Estimates for these variables were obtained by optimizing ("tuning") these variables to obtain close agreement of HYDRUS-simulated and field 1 ISC-estimated flux and under-tarp fumigant gas data.

Although limited laboratory data exist for 1,3-D and chloropicrin Raven VaporSafe™ permeabilities (Qian et al., 2011), we treated the HYDRUS tarp permeability factor *d* as a "field averaged" parameter, independent of temperature. There are several reasons for this approach. First, it's apparent that laboratory permeability data do not accurately reflect actual permeability in the field. The first order model used in laboratory tarp permeability measurement relates flux density through the tarp to the concentration difference across the tarp (Paperniek et al., 2011).

$$[1] \qquad J = -k_{MTC}\ (C_R - C_S)$$

where J = flux density (ug cm^{-2} h^{-1}), k_{MTC} is a first-order mass transfer coefficient (cm h^{-1}), C_R is fumigant concentration on the receiving side of the tarp (ug cm^{-3}, usually assumed = 0 for field data) and C_S is the concentration on the source side of the tarp. Using Eq. 1, maximum undertarp chloropicrin concentrations, and peak flux data, effective chloropicrin-Raven VaporSafe^{TM} TIF k_{MTC} s based on field data are in the range of 0.1 cm h^{-1} (data of Qin et al., 2011) to 0.3 cm h^{-1} (field 1 data reported here). These effective field k_{MTC}s are more than 2 orders of magnitude greater than the laboratory-measured chloropicrin-Raven VaporSafe^{TM} k_{MTC} of 0.0005 (Qian et al., 2011; 25˚C, 90% relative humidity). Secondly, relative humidity (RH) has been shown to have a dramatic effect on tarp permeability in some cases (Paperniek et al, 2010; Qian et al., 2011). Since the functional relationship between permeability and RH is unknown, use of an average tarp permeability over the time course of the study was deemed a logical approach. Third, there is little permeability versus temperature data for Raven VaporSafe^{TM} tarps, limiting our ability to accurately parameterize HYDRUS independently. When the tarp is rolled out onto the soil during application, small rips, stretched zones or glued zones may be created which increases diffusion of fumigant through the tarp compared to laboratory-measured permeability which utilizes only intact tarp samples. Finally, HYDRUS does have the ability to simulate tarp permeability-temperature effects. However, initial attempts to estimate the tarp activation energy (dE_a, which describes permeability temperature dependence) yielded little improvement in model fits to the ISC-estimated flux data; there was little reduction in the calibration objective function (Eq. [2], below), and 95% confidence intervals about the optimized dE_a included zero.

Simulation of tarp cutting/removal

Actual tarp removal in the field is a two-stage process. The tarp is usually cut using small all-terrain vehicles with trailing knives that make a rapid length-wise pass over every tarp panel, slicing them in the process. After 24 hours, the tarp is then completely removed. HYDRUS is capable of simulating dual volatilization boundary conditions where part of the surface has a mass transfer resistance (i.e. is “tarped”) and the remainder is bare ground. Thus, in theory the model is capable of simulating both a cut tarp condition (dual volatilization boundary condition) and subsequent tarp removal (i.e. elimination of the tarp resistance entirely in mid-simulation). In practice there is no way to determine what portion of the soil surface should be treated as untarped when simulating a cut tarp condition. Because cut tarps often “flutter,” even under relatively light wind conditions, there is no accurate way to simulate a cut tarp. Consequently the tarp cutting/removal process was simulated as instantaneous complete removal in all simulations.

Calibration procedure

The nonlinear optimization program PEST (Doherty, 2004) was used to determine “best-fit” values of k_1, d and K_{OC} for both chloropicrin and 1,3-D. An iterative step-wise optimization procedure was used to optimize the three variables.

1. Select an initial K_{OC} value from literature, calculate fumigant soil-water partition coefficients K_d (ml g^{-1}) for each soil layer as $K_d = K_{OC}\ x\ OC$.

2. With the K_d estimates from step 1, use PEST to determine k_1 and d that minimize Φ_1 (Eq. 2).

$$[2] \qquad \Phi_1 = \sum_{i=2}^{42} [\frac{(F_{HYDRUS,i} - F_{ISC,i})^2}{\sigma^2_{F,ISC}} + \frac{(f_{HYDRUS,i} - f_{ISC,i})^2}{\sigma^2_{f,ISC}}]$$

   where $F_{HYDRUS,i}$ is the HYDRUS-simulated cumulative flux after period i, $F_{ISC,i}$ is the ISC-estimated cumulative flux after period i, $\sigma^2_{F,ISC}$ is the variance of the ISC period 2 – 42 cumulative fluxes, $f_{HYDRUS,i}$ is the HYDRUS-simulated period mean flux density for period i, $f_{ISC,i}$ is the ISC-estimated period mean flux density for period i, and $\sigma^2_{f,ISC}$ is the variance of the ISC periods 2 – 42 mean flux densities. The variances are weighting factors for the cumulative flux and discrete flux sum of squares terms that correct for scale differences.

3. "Freeze" k_1 and d at the values obtained in the previous step. Using repeated HYDRUS simulations, determine the mean simulated surface (undertarp) fumigant soil gas concentrations for pre-tarpcut gas sampling events (times = 1.4, 2.4, 3.4, 6.4, 9.4, 12.4, and 15.4 d) for a range of different K_{OC}s. The mean undertarp gas concentration at each time was calculated as the mean of soil surface gas concentration determined at 2 cm intervals across the top of the modeling domain. Using these data, determine the value of K_{OC} that yields the minimum value of Φ_2 (Eq. 3).

$$[3] \qquad \Phi_2 = \sum_{i=1}^{7} (\overline{g}_{HYDRUS,i} - \overline{g}_{meas,i})^2$$

   where $\overline{g}_{HYDRUS,i}$ is the mean simulated surface fumigant gas concentration for gas sampling event i and $\overline{g}_{meas,i}$ is the mean measured surface fumigant gas concentration for gas sampling event i (n=24 for each of the 7 pre-tarpcut surface gas sampling events).

4. Repeat step 2 using the K_{OC} obtained in 3 above, then repeat step 3. Continue iterating using steps 2 and 3 until best-fit values for k_1, d and K_{OC} converge. We achieved convergence of all 3 variables within 4 iterations based on a criterion of < 3% change in estimates between iterations.

In contrast to the step-wise calibration summarized above, a single-step optimization that included cumulative flux, flux density *and* soil-gas concentration in the optimization function Φ_1 generally yielded optimized variables with much larger confidence limits, and poorer cumulative flux and flux density model predictions relative to the step-wise procedure. This was

likely due to a larger number of variables being optimized (3 versus 2), the variability in the soil-gas data, and the effect of large scale differences among the cumulative flux, flux density and soil gas concentration data.

RESULTS

Calibration Results

The calibration yielded optimized parameters that generally compared favorably to published values (Table 2). Degradation rate constants for chloropicrin and 1,3-D corresponded to half-lives of 4.3 and 7.2 d, respectively. Wilhelm et al. (1996) reported a chloropicrin half-life of 4.5 d, while 1,3-D aerobic soil half-lives range from 4.2 – 18.7 days (van Dijk, 1980). Ranges in organic carbon-normalized soil partition coefficients for chloropicrin and 1,3-D are 2 – 82 and 32 – 98 ml g^{-1}, respectively (USDA-ARS pesticide properties database, <http://www.ars.usda.gov/Services/docs.htm?docid=14195>). Our optimized K_{OC} s for the two fumigants fall within or are close to these reported ranges (Table 3).

The best-fit boundary layer depths in Table 3 correspond to k_{MTC} s of 0.12 and 0.22 cm h^{-1} for chloropicrin and 1,3-D, respectively, where $k_{MTC} = D_g/d$ (D_g = gas phase diffusion coefficient, 287 and 271 cm^2h^{-1} for 1,3-D and chloropicrin, respectively). Mean post-study Raven Vaporsafe^{TM} k_{MTC} s measured in the laboratory were 0.02 and 0.06 cm h^{-1} for chloropicrin and 1,3-D, respectively (N=3; Gao et al., 2013). The differences between field and laboratory k_{MTC} s are not large, and may be attributable to intrinsic differences in laboratory versus effective field permeabilities, representativeness of the 3 tarp samples, or temperature effects. The laboratory measurements were conducted at 22 ^oC, whereas undertarp temperatures in the Lost Hills study ranged from 12 ^oC to 77 ^oC during the field 1 study period (Figure A-1, Appendix).

Table 2. Field 1 HYDRUS calibration results: optimized variables and 95% CI.

variable	chloropicrin	1,3-D
k_1 (d^{-1})	0.1595 (0.1413, 0.1777)	0.0965 (0.0908, 0.1029)
K_{OC}	66 [A]	30 [A]
d (cm)	2230 (1925, 2534)	1326 (1233, 1421)

[A] Confidence intervals not determined

HYDRUS simulated cumulative fluxes compared favorably with the ISC inverse modeled estimates (Figure 2, Table 3). The cumulative flux as a fraction of applied mass for chloropicrin was 0.043 and 0.042 and 0.099 and 0.096 for 1,3-D, ISC- and HYDRUS-estimated, respectively. These differences in emission ratios (ISC – HYDRUS) are 0.001 (2.5%) and 0.003 (2.6%), respectively, for chloropicrin and 1,3-D.

Differences in maximum discrete period-mean pre-tarpcut flux densities were greater, with percent differences of 5% and -13% for chloropicrin and 1,3-D, respectively (percent

difference = (ISC-HYDRUS)/ISC*100; Figure 3). While HYDRUS reproduced the general magnitudes and diurnal variations in the pre-tarpcut discrete ISC-estimated flux densities, the timing of the peak discrete fluxes was one day later in the simulated as compared to the ISC estimates. Simulated and inverse modeled post-tarpcut discrete fluxes were comparable, providing evidence that the simulated degradation rate of the two fumigants were accurately represented.

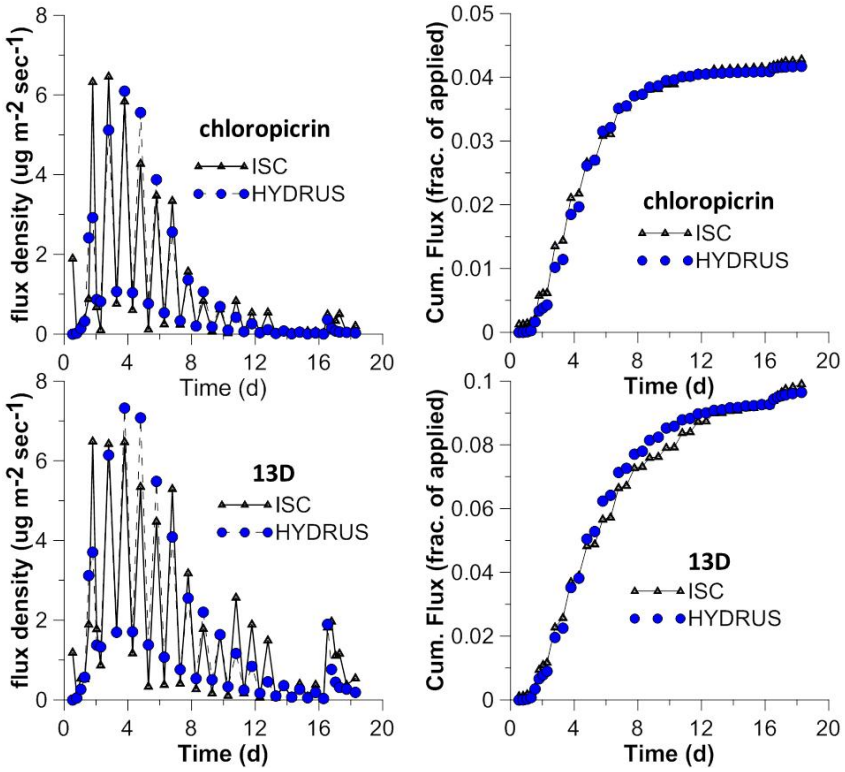

Figure 3. Chloropicrin and 1,3-D period mean flux densities and cumulative flux from field 1 calibration.

In addition to fumigant volatilization and degradation, fumigant air-water partitioning, heat transport and water content dynamics were well-described by the calibrated model. While there were small systematic deviations between measured and simulated soil temperature at the deeper depths, the differences were relatively small with a maximum deviation between measured and simulated soil temperature at 70 cm of 1.7˚C late in the study (Figure 4). The measured soil temperature data at each depth are the average of two measurements in the surrogate plot adjacent to field 1 (Figure 1), and default thermal conductivity parameters were used in the simulation (Horton and Chung, 1991).

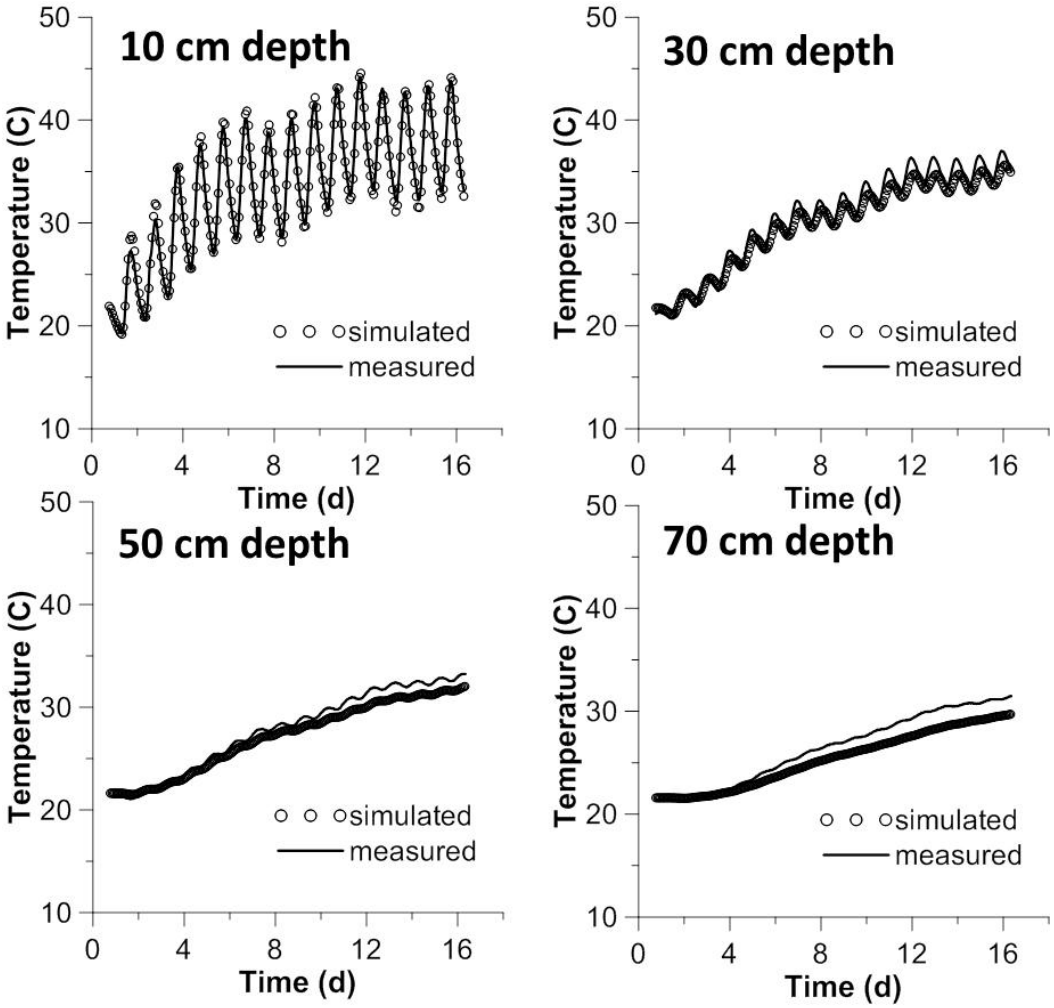

Figure 4. HYDRUS-simulated and measured temperatures at four soil depths. Measured undertarp surface temperature (depth = 0 cm) was used as a boundary condition in the simulations.

The magnitude and dynamics of simulated soil gas concentrations were generally consistent with the measured data, but there was a tendency early in the simulation to underestimate surface concentrations and overestimate concentrations at the 25 cm depth close to the application zone (Figure 5). Both observations are consistent with the delay in HYDRUS simulated flux data previously discussed, indicating a tendency for delayed simulated transport from the zone of application to the surface relative to actual transport in the field.

chloropicrin **1,3-D**

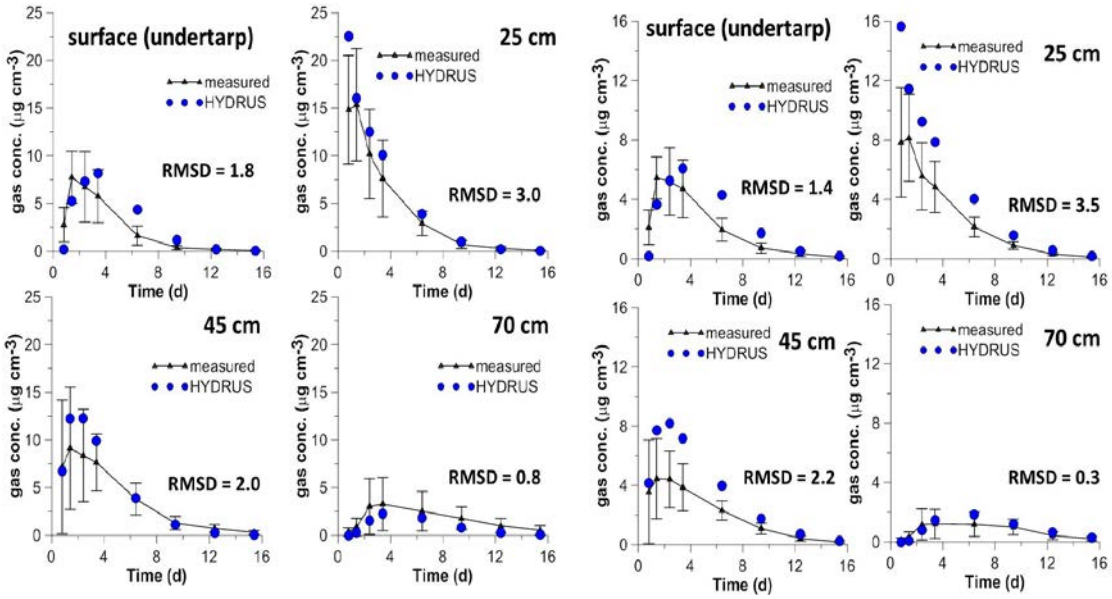

Figure 5. Simulated and measured fumigant gas phase concentrations undertarp and at 25, 45, and 70cm depths. Error bars are standard deviations; n=24 samples at each time for surface samples; n=12 samples at each time for 25, 45 and 70 cm deep samples. RMSD = root mean square deviation between simulated data and means of measured data at each depth.

There was little water content change in field 1 over the course of the study, and simulated end of study water contents agreed well with the measured data (Figure 6).

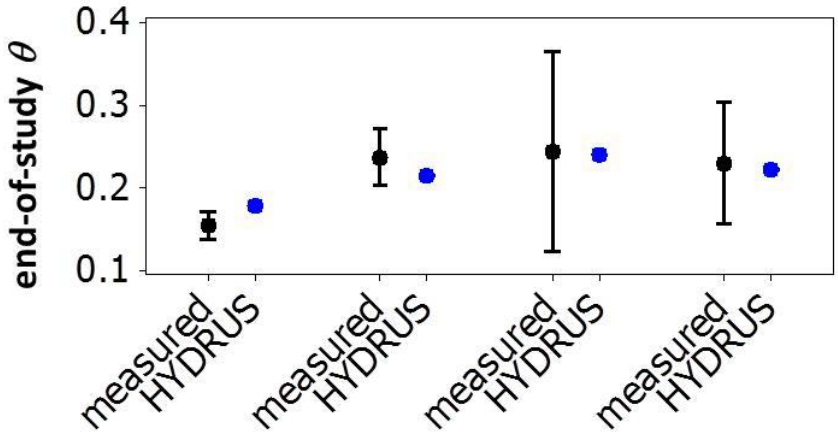

Figure 6. Measured (N=4) and simulated end of study water contents for field 1. Error bars are 95% confidence intervals for the mean.

Mass budgets were developed for the field data and HYDRUS simulation (Table 3) using the ISC-estimated fluxes and end of study soil gas concentrations measured down to the 100 cm depth. The corresponding HYDRUS mass budgets predicted that nonvolatilized fumigant was almost entirely degraded over the study period, with only a small fraction moving deeper in the profile over the 18.4 d study period.

Table 3. Field 1 mass budgets for field data and HYDRUS simulations.

1,3-D	**Field data** [A]	**HYDRUS**
Volatilized	9.9%	9.6%
Remaining at 18 days (0-100cm)	1.0%	0.9%
Degraded or deep transport (>100cm)	89.1%	89.5%
Degraded	---- [B]	89.1%
Transport beyond 100cm	----	0.4%
Numerical error	----	-0.04%
CHLOROPICRIN		
Volatilized	4.3%	4.2%
Remaining at 18 days (0-100cm)	1.0%	0.1%
Degraded or deep transport (>100cm)	94.7%	95.9%
Degraded	----	95.8%
Transport beyond 100cm	----	0.1%
Numerical error	----	-0.12%

[A] **"**Volatilized" estimated by ISC inverse modeling of off-site fumigant air concentrations; fumigant "remaining at 18 days" calculated from soil gas concentration, K_{OC}, OC, , temperature-adjusted K_H and end of study water content; total (degraded + deep transport) by difference.

[B] Field data can't discern between degradation and deep transport

Simulation of Field 2 and Field 3 Flux Data

Field 2 and field 3 chloropicrin and 1,3-D fluxes were simulated using measured application rates and soil properties for those fields, and the k_1, d and K_{OC} calibrated from the field 1 data (Table 2). Thus, all model input data for fields 2 and 3 were determined independent of the simulations; no "tuning" of the variables was performed.

HYDRUS simulated field 2 and 3 cumulative fluxes well, with mean absolute differences in simulated and inverse modeled emission ratios (cumulative flux mass/applied fumigant mass) of 0.009 and 0.026 for chloropicrin and 1,3-D, respectively (Figures 7,8, Tables 4 and 5). Simulated field 2 and 3 maximum pre-tarpcut discrete flux densities also compared favorably to the ISC inverse-modeled estimates, with mean percent difference of 30% (chloropicrin) and 17% (1,3-D) (Table 4). These differences are likely within the range of uncertainty of the ISC inverse modeling procedure as discussed in the Introduction. However, timing of the simulated

maximum flux densities were delayed compared to the ISC inverse-modeled estimates; HYDRUS pre-tarpcut maximum discrete flux densities occurred two days later than the ISC estimated maximum flux densities in 3 of the 4 comparisons (Figures 7, 8).

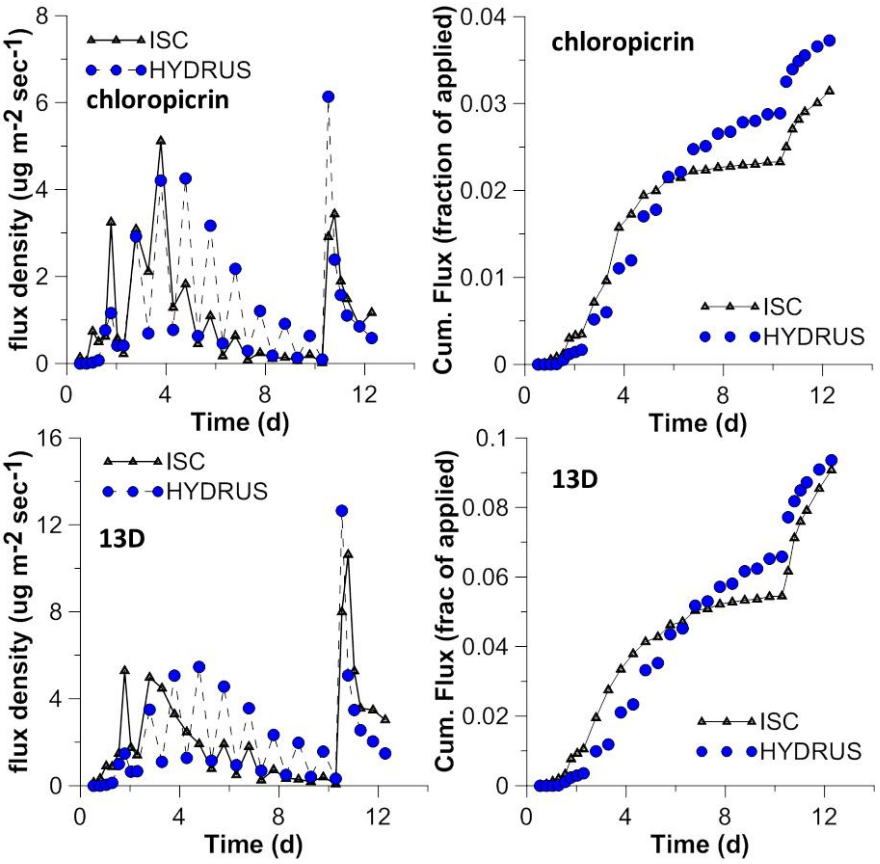

Figure 7. Chloropicrin and 1,3-D period mean flux densities and cumulative flux for field 2. ISC estimates derived from inverse modeling of measured off-site air concentrations.

Post-tarpcut maximum flux densities differed by 56% (chloropicrin) and 13% (1,3-D) between the two methods. The relationship between modeled post-tarpcut maximum flux density and tarp holding time closely tracked that of the ISC estimates (Figure 9). These estimates spanned more than an order of magnitude in range.

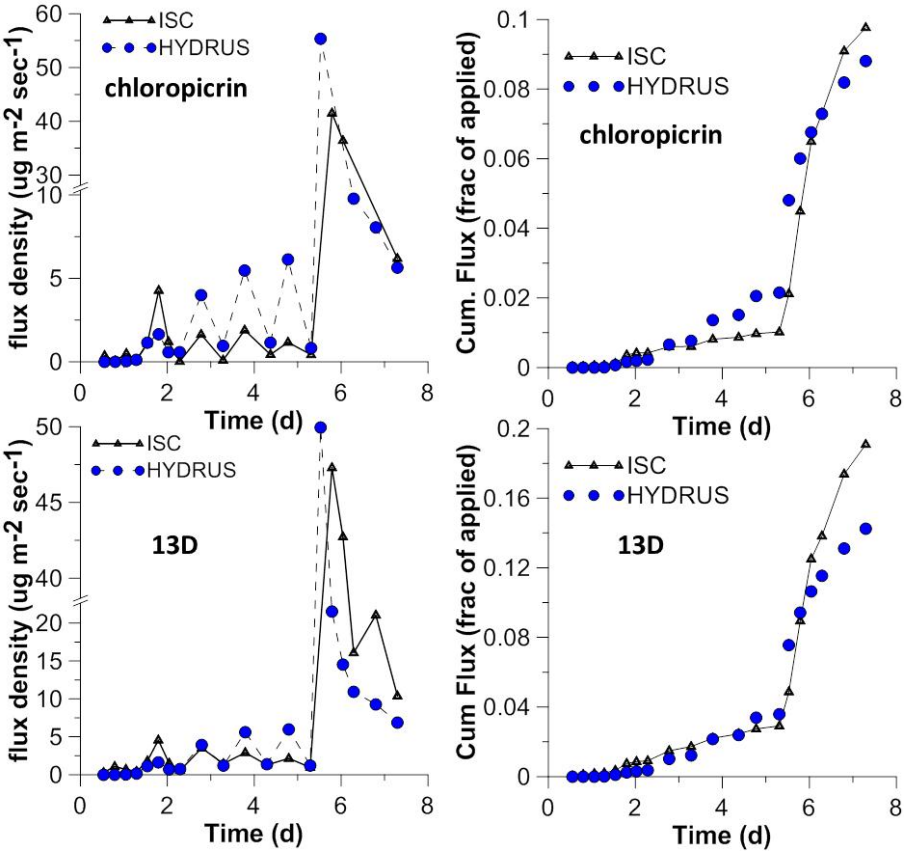

Figure 8. Chloropicrin and 1.3-D period-mean flux densities and cumulative flux for field 3. ISC estimates derived from inverse modeling of measured off-site air concentrations. Note broken axes on chloropicrin and 1,3-D discrete period mean flux density plots.

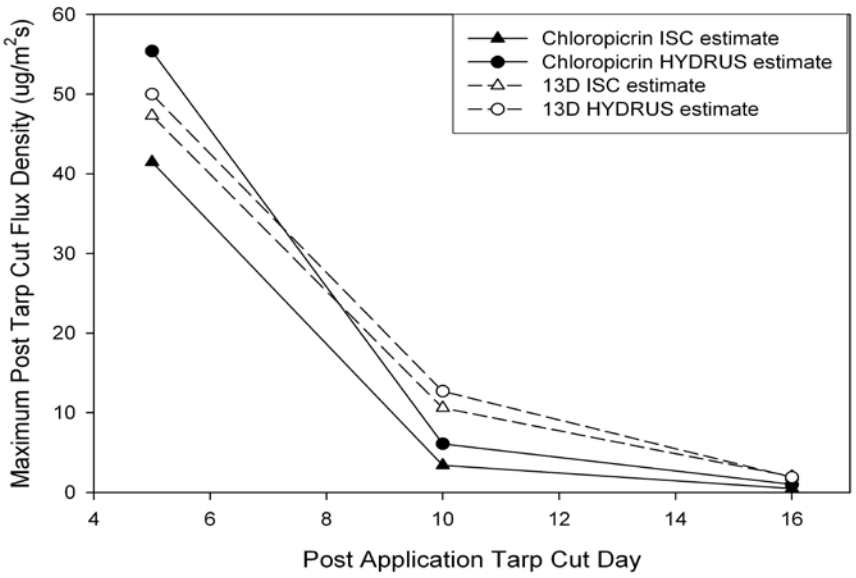

Figure 9. HYDRUS- and ISC-estimated maximum six hour post-trarpcut flux densities for chloropicrin and 1,3-D for tarp holding times of 5 d (field 3), 10 d (field 2) and 16 d (field 1).

Table 4. Pre-tarpcut mean absolute emission ratio (ER) difference and percent difference in maximum discrete flux densities between ISC inverse modeled and HYDRUS simulations.

CHLOROPICRIN	Field 1	Field 2	Field 3	
Emission Ratio to tarpcut				mean absolute ER difference[A]
ISC	0.042	0.023	0.010	
HYDRUS	0.041	0.029	0.022	**0.009**
pre-tarpcut max flux (ug/m^2 sec)				mean absolute PERCENT difference[A]
ISC	6.5	5.1	4.3	
HYDRUS	6.2	4.3	6.1	**30%**
13D	**Field 1**	**Field 2**	**Field 3**	
Emission Ratio to tarpcut				mean absolute ER difference[A]
ISC	0.092	0.055	0.029	
HYDRUS	0.092	0.066	0.036	**0.009**
pre-tarpcut max flux (ug/m^2 sec)				mean absolute PERCENT difference[A]
ISC	6.5	5.3	4.6	
HYDRUS	7.3	5.5	6.0	**17%**

[A] based on fields 2 and 3 ISC/HYDRUS data comparisons; maximum flux densities determined across 6 hour AND 12 hour period mean flux densities. Absolute percent difference = | (ISC-HYDRUS)/ISC | *100.

Table 5. Mean absolute end-of-study emission ratio (ER) difference and percent difference in post-tarpcut maximum discrete flux densities between ISC inverse modeled and HYDRUS simulations.

CHLOROPICRIN	Field 1	Field 2	Field 3	
Emission ratio to end-of-study				mean absolute ER difference[A]
ISC	0.043	0.031	0.098	
HYDRUS	0.042	0.039	0.088	**0.009**
post-tarpcut max flux (ug/m^2 sec)				mean absolute PERCENT difference[A]
ISC	0.5	3.4	41.5	
HYDRUS	1.0	6.1	55.4	**56%**
13D	Field 1	Field 2	Field 3	
Emission ratio to end-of-study				mean absolute ER difference[A]
ISC	0.099	0.091	0.191	
HYDRUS	0.096	0.094	0.143	**0.026**
post-tarpcut max flux (ug/m^2 sec)				mean absolute PERCENT difference[A]
ISC	2.0	10.6	47.3	
HYDRUS	1.9	12.7	50.0	**13%**

[A] based on fields 2 and 3, ISC/HYDRUS data comparisons. All comparisons are between 6 h mean flux densities. Absolute percent difference = | (ISC-HYDRUS)/ISC | *100.

Both flux estimation methods (ISC and HYDRUS) yielded much lower period mean flux densities and cumulative fluxes as compared to PE tarp applications; application rate normalized period mean flux densities for PE tarps are a factor of 5*x* to 10*x* greater than the estimates for TIF obtained in this study (Table 6).

Table 6. Maximum period mean flux densities (ug m^{-2} s^{-1}) normalized to 100 lbs $acre^{-1}$ applied for ISC- and HYDRUS-estimated Lost Hills TIF applications and PE tarp applications reported in the literature.

data source	normalized chloropicrin flux density	normalized 1,3-D flux density
Lost Hills Field 1 – ISC – TIF	1.9[A]	2.8[B]
Lost Hills Field 2 – ISC – TIF	1.6[A]	2.4[B]
Lost Hills Field 3 – ISC – TIF	1.5[B]	2.3[B]
Lost Hills Field 1 – HYDRUS – TIF	1.8[A]	3.2[A]
Lost Hills Field 2 – HYDRUS – TIF	1.3[A]	2.5[A]
Lost Hills Field 3 – HYDRUS – TIF	1.7[A]	2.5[A]
Qin et al. (2011) – PE	10.2[C]	21.3[C]
Gao et al. (2008) – PE	10.5[C]	15.1[C]

[A] 12 hour mean flux density
[B] 6 hour mean flux density
[C] 3 hour mean flux density

CONCLUSION

The calibrated HYDRUS model estimates of cumulative flux and magnitude of post tarpcut fumigant "flush" were comparable to those estimated by ISC. The magnitude of HYDRUS-simulated maximum period mean flux densities were within the likely uncertainty of the ISC inverse modeled estimates. Based on the field 1 soil-gas data, soil temperature data, end of study soil-water content data, and post-tarpcut fluxes, HYDRUS accurately simulated the actual heat transport, partitioning and degradation processes that occurred in the field. Individual process simulation is critical because of the potential for complex nonlinear models to yield desirable results, even though individual processes may not be accurately described. Without accurate process simulation, confidence in model extrapolations to other conditions is limited. Using the end-of-study soil gas data, a field mass budget was developed. Approximate agreement in estimated post-study fumigant (degradation+deep transport) provided additional evidence that the simulated mass budget reflected actual fumigant fate in the field.

HYDRUS displayed a tendency for delayed, or slow, transport from the zone of application to the soil surface. This was evidenced by model predictions of initially low fumigant gas-phase surface concentrations in field 1 simulations, and maximum period mean flux densities delayed by one to two days relative to ISC inverse modeled estimates in five of six simulations. Several factors may contribute, including error in the semi-empirical tortuosity model used to describe effective soil diffusion, or inaccurate specification of model initial conditions with regard to fumigant distribution in soil. The simulations here assumed two adjacent initial fumigant concentration zones 10 cm in vertical thickness, centered at the 30 cm depth of application, each with a lateral width equal to Nobel plow wing width of ~ 90 cm. Finally, a vertical column of low bulk density soil resulting from passage of the plow shank could also have contributed to more rapid upwards diffusion in the field relative to model simulations. However, an ancillary study conducted at Lost Hills concluded that this putative “shank trace” effect was probably only of minor importance, if any (Johnson, 2012).

REFERENCES

Ajwa, H; D.A. Sullivan. 2012. Soil Fumigant Emissions Reduction using EVAL barrier resin film (VaporSafe™) and Evaluation of Tarping Duration Needed to Minimize Fumigant Total Mass Loss. Study ID HA2011A submitted to DPR, 404 pp.

Carsel, R.F. and R.S. Parrish. 1988. Developing Joint Probability Distributions of Soil Water Retention Characteristics. Water Resources Research 24:755-769.

Chickos, J.S. and W.E. Acree, Jr. 2003. Enthalpies of Vaporization of Organic and Organometallic Compounds, 1880–2002. J. Phys. Chem. Ref. Data, Vol. 32: 519-878.

Doherty, J. 2004. PEST: Model-Independent Parameter Estimation and Uncertainty Analysis. Ver. 5. Watermark Computing.

Dungan, R.S. and S.R. Yates. 2003. Degradation of Fumigant Pesticides: 1,3-Dichloropropene, Methyl Isothiocyanate, Chloropicrin, and Methyl Bromide. Vadose Zone J. 2:279-286.

Gan, J., S.R. Yates, F.F. Ernst, and W.A. Jury. 2000a. Degradation and Volatilization of the Fumigant Chloropicrin after Soil Treatment. Environ. Qual. 29:1391–1397.

Gao, S., Ajwa, H., Qin, R., Stanghellini, M. and D. Sullivan. 2013. Emission and Transport of 1,3-Dichloropropene and Chloropicrin in a Large Field Tarped with VaporSafe™ TIF. Environ. Sci. Technol. 47: 405−411.

Gao, S., T.J. Trout and S. Schneider. 2008. Evaluation of Fumigation and Surface Seal Methods on Fumigant Emissions in an Orchard Replant Field. J. Env. Qual. 37:369–377.

Hilal, S.H., S.W. Karickhoff and L.A. Carreira. 2003a. Prediction of Chemical Reactivity Parameters and Physical Properties of Organic Compounds from Molecular Structure using SPARC. USEPA publication 600/R-03/030. Available at: <http://www.epa.gov/athens/publications/reports/EPA_600_R03_030.pdf>.

Hilal, S.H., S.W. Karickhoff and L.A. Carreira. 2003b. Verification and Validation of the SPARC Model. USEPA publication 600/R-03/033. Available at: <http://www.epa.gov/athens/publications/reports/EPA_600_R03_033.pdf>.

Horton, R. and S. Chung. 1991. Soil Heat Flow. In: J. Hanks and J.T. Ritchie (Editors), Modeling Plant and Soil Systems. American Society of Agronomy, Inc., Madison, WI, pp. 397-438.

Hsieh, D.P.H., Seiber, J.N., and J.E. Woodrow. 1995. Development of Predictive Methods for Estimating Pesticide Flux to Air, Part 2. Final Report to California Air Resources Board, Research Division, 92-313. UC Davis, Dept. Environ. Tox.

Johnson, B. 2012. Bulk density associated with shank trace in fumigant application. *in preparation*.

Johnson, B. and F. Spurlock. 2013. Stochastic Evaluation of Back Calculation Procedures for Estimating Flux Using Data From the Lost Hills Study. Environ. Monitoring, Ca. Dept. Pest. Reg. <http://www.cdpr.ca.gov/docs/emon/pubs/ehapreps/analysis_memos/2415_segawa.pdf>.

Johnson, B., Barry, T., and P. Wofford. 2010. Workbook for Gaussian Modeling Analysis of Air Concentration Measurements. Environ. Monitoring, Ca. Dept. Pest. Reg., on-line: <http://www.cdpr.ca.gov/docs/emon/pubs/ehapreps/analysis_memos/4559_sanders.pdf>.

Kawamoto,K., and K. Urano. 1989. Parameters for predicting fate of organochlorine pesticides in the environment (I) Octanol-water and air-water partition coefficients. Chemosphere 18:1987-1996.

Majewski, M.S., 1996. Error evaluation of methyl bromide aerodynamic flux measurements. In: Seiber, J.N., Knuteson, J.A., Woodrow, J.E., Wolf, N.L., Yates, M.V., Yates, S.R. (Eds.), Fumigants: Environmental Fate, Exposure, and Analysis.ACS Symposium Series, vol. 652. American Chemical Society, Washington, DC, pp. 135}153.

Papiernek, S.K., Yates, S.R., Chellimi, D.O. 2011. A standardized approach for estimating the permeability of plastic films to soil fumigants under various field and environmental conditions. J. Environ. Qual. 40: 1375-1382.

Parmele, L.H., Lemon, E.R., and A.W. Taylor. 1972. Micrometeorological measurement of pesticide vapor flux from bare soil and corn under field conditions. Water, Air, and Soil Poll 1:433-451.

Qian,Y., Kamel, A., Stafford, C., Nguyen, T., Chism, W.J., Dawson, J., and C. W. Smith. 2011. Evaluation of the Permeability of Agricultural Films to Various Fumigants. Environ. Sci.Technol. Environ. Sci. Technol. 45:9711–9718.

Qin, R., Gao, S., Ajwa, H., Sullivan, D., Wang, D. and B. D. Hanson. 2011. Field Evaluation of a New Plastic Film (Vapor Safe) to Reduce Fumigant Emissions and Improve Distribution in Soil. J. Environ. Qual. 40:1195–1203.

Ross, L.J., Johnson, B., Kim, K.D., Hsu, J., 1996. Prediction of methyl bromide flux from area sources using the ISCST model. Journal of Environmental Quality 25 (4), 885-891.

Sax, T. and V. Isakov. 2003. A case study for assessing uncertainty in local-scale regulatory air quality modeling applications. Atmosph. Environ. 37:3481-3489.

Spurlock, F., Šimůnek, J., Johnson, B. and A. Tuli. 2012. Sensitivity Analysis of Soil Fumigant Transport and Volatilization to the Atmosphere. Vadose Zone Journal. doi:10.2136/vzj2012.0130.

Sullivan, D.A., Holdsworth, D.J., and D.J. Hlink. 2004. Monte Carlo-based dispersion modeling of off-gassing releases from the fumigant metam-sodium for determining distances to exposure endpoints. Atmos. Environ. 38:2471–2481.

Tuli, A. 2011. Modeling and Monitoring Field Emissions of Fumigants Under Totally Impermeable Films (TIF).Protocol for Study 273. Environ. Monitoring, Ca. Dept. Pest. Reg., on-line: <http://www.cdpr.ca.gov/docs/emon/pubs/protocol/study273protocol.pdf>.

van Dijk, H. 1980. Dissipation Rates in Soil of 1,2-Dichloropropane and 1,3- and 2,3-Dichloropropenes. Pestic. Sci. 11:625–632.

van Genuchten, M. Th. 1980. A Closed-form Equation for Predicting the Hydraulic Conductivity of Unsaturated Soils. Soil Sci. Soc. Am. J., 44:892-898.

van Genuchten, M. Th., F. J. Leij, and S. R. Yates. 1991. The RETC Code for Quantifying the Hydraulic Functions of Unsaturated Soils, Version 1.0. EPA Report 600/2-91/065, U.S. Salinity Laboratory, USDA-ARS, Riverside, California.

Wang, D., S. Gao, R. Qin, and G. Browne. 2010. Lateral Movement of Soil Fumigants 1,3-Dichloropropene and Chloropicrin from Treated Agricultural Fields. J. Env. Qual. 39:1800–1806.

Wang, L., Parker, D.B., Parnell, C.B., Lacey, R.E., and B.W. Shaw. 2006. Comparison of CALPUFF and ISCST3 models for predicting downwind odor and source emission rates. Atmos. Environ. 40:4663–4669.

Wilhelm, S.N., K. Shepler, L.J. Lawrence, and H. Lee. 1996. Environmental Fate of Chloropicrin. p. 79–93. In J.N. Seiber et al. (ed.) Yates, S.R., D. Wang, F.F. Ernst, and J. Gan. 1997. Ser. 652. American Chemical Society, Washington, DC.

Wright, D.A., Sandler, S.I. and D. DeVoll. 1992. Infinite dilution activity coefficients and solubilities of halogenated hydrocarbons in water at ambient temperatures. Environ. Sci. Technol. 26:1928-1931.

APPENDIX – LOST HILLS HYDRUS SIMULATIONS

Table A-1. Soil data used in HYDRUS simulations. Soil properties between 80 and 150 cm were assumed identical to layer 4 (60 – 80 cm) properties.

Input Variable (units)	Variable name	Layer 1	Layer 2	Layer 3	Layer 4
Field 1					
ρ_b ($cm^3 g^{-1}$)	soil bulk density	1.474	1.189	1.527	1.381
θ_s (-)	saturated water content	0.545	0.445	0.442	0.446
θ_i (-)	initial water content	0.172	0.216	0.241	0.219
θ_r (-)	residual water content	0.039	0.039	0.039	0.039
α (cm^{-1})	VG retention model parameter	0.15796	0.057833	0.04505	0.05552
n (-)	VG retention model parameter	1.2427	1.22544	1.19846	1.2108
OC (g OC g^{-1})	soil organic carbon	0.60	0.50	0.00	0.00
Field 2					
ρ_b $cm^3 g^{-1}$	soil bulk density	1.264	1.471	1.504	1.396
θ_s (-)	saturated water content	0.523	0.4453	0.43275	0.4735
θ_i (-)	initial water content	0.205	0.272	0.311	0.319
θ_r (-)	residual water content	0.039	0.039	0.039	0.039
α (cm^{-1})	VG retention model parameter	0.14919	0.036693	0.02318	0.100313
n (-)	VG retention model parameter	1.18572	1.1959	1.17462	1.13549
OC (g OC g^{-1})	soil organic carbon	0.66	0.45	0.15	0.12
Field 3					
ρ_b $cm^3 g^{-1}$	soil bulk density	1.288	1.464	1.51	1.379
θ_s (-)	saturated water content	0.514	0.4475	0.430	0.483
θ_i (-)	initial water content	0.213	0.262	0.299	0.313
θ_r (-)	residual water content	0.039	0.039	0.039	0.039
α (cm^{-1})	VG retention model parameter	0.265982	0.144417	0.114204	0.04287
n (-)	VG retention model parameter	1.19079	1.14313	1.15657	1.19182
OC (g OC g^{-1})	soil organic carbon	0.59	0.45	0.21	0.17

Table A-2. Principal input variables required for HYDRUS simulations.

Input Variable (units)	Variable name	Source
ρ_b ($cm^3(gm\ soil)^{-1}$)	soil bulk density[A]	measured
θ_s (-)	saturated water content[A]	calculated from bulk density ($\theta_s = 1 - \rho_b/2.65$)
θ_i (-)	initial water content[A]	measured
θ_r (-)	residual water content[A]	sandy loam texture class mean (Carsel and Parrish, 1988)
α (cm^{-1})	VG retention model parameter[A, B]	measured
n (-)	VG retention model parameter[A, B]	measured
K_s (cm d^{-1})	saturated hydraulic conductivity[A]	sandy loam texture class mean (Carsel and Parrish, 1988)
C_n (J cm^3 K^{-1})	volumetric solid phase heat capacity[A]	HYDRUS default
λ_L, b_1, b_2, b_3	soil thermal conductivity parameters[A]	Chung and Horton (1980)
$T_0(t)$ (C)	soil surface temperature as function of time *t*	measured – surrogate field plot
D_g (cm^2 d^{-1})	gas phase diffusion coefficient	SPARC on-line calculator (Hilal et al., 2003a, 2003b)
D_gE_a (J mol^{-1})	D_g activation energy[C]	SPARC on-line calculator (Hilal et al., 2003a, 2003b)
D_w (cm^2 d^{-1})	aqueous phase diffusion coefficient	SPARC on-line calculator (Hilal et al., 2003a, 2003b)
D_wE_a (J mol^{-1})	D_w activation energy[C]	SPARC on-line calculator (Hilal et al., 2003a, 2003b)
K_h (-)	Henry's law constant	*chloropicrin:* Kawamoto and Urano (1989); *1,3-D*: Wright, (1992)
K_hE_a (J mol^{-1})	K_h activation energy[C]	*chloropicrin:* Chikos and Acree (2006); *1,3-D*: Wright, (1992)
k_1 (d^{-1})	first-order degradation rate constant[A]	**calibrated**
k_1E_a (J mol^{-1})	k_1 activation energy[A,C]	mean [data of Dungan et al. (2003) and Gan et al. (2000)]
OC (g OC (g $soil^{-1}$)	soil organic carbon mass fraction[A]	measured
K_d (ml^3 g^{-1})	soil partition coefficient[A]	calculated from **calibrated** K_{OC} and measured OC ($K_d = K_{OC}$ * OC)
d (cm)	tarp boundary layer depth[D]	**calibrated**
λ_w (cm)	longitudinal dispersivity	HYDRUS default

[A] required for each soil layer

[B] van Genuchten (VG) soil-water retention model was used (van Genuchten, 1980)

[C] activation energies describe the temperature dependence of the associated parameter (Spurlock et al., 2012)

[D] tarp boundary layer depth (describes tarp permeability) assumed independent of temperature – see calibration discussion.

Table A-3. Chemical Property Input variables used for HYDRUS simulations.

Input Variable (units)	**Variable name**	**Source**
D_g (cm^2 d^{-1})	gas diffusion coefficient *chloropicrin:* 6515 *13D:* 6886	SPARC on-line calculator (Hilal et al., 2003a, 2003b)
D_gE_a (J mol^{-1})	D_g activation energy *chloropicrin:* 4566 *13D:* 4560	SPARC on-line calculator (Hilal et al., 2003a, 2003b)
D_w (cm^2 d^{-1})	aq. diffusion coefficient *chloropicrin:* 0.707 *13D:* 0.735	SPARC on-line calculator (Hilal et al., 2003a, 2003b)
D_wE_a (J mol^{-1})	D_w activation energy *chloropicrin:* 17920 *13D:* 18035	SPARC on-line calculator (Hilal et al., 2003a, 2003b)
K_h (-)	Henry's constant. *chloropicrin:* 0.083 *13D:* 0.050	*chloropicrin:* Kawamoto and Urano (1989); *1,3-D*: Wright, (1992)
K_hE_a (J mol^{-1})	K_h activation energy *chloropicrin:* 39120 *13D:* 32085	*chloropicrin:* Chikos and Acree (2006); *1,3-D*: Wright, (1992)
k_1 (d^{-1})	degradation constant *chloropicrin:* 0.1595 *13D:* 0.0968	**calibrated from field 1 data**
k_1E_a (J mol^{-1})	k_1 activation energy *chloropicrin:* 56933 *13D:* 59028	mean [data of Dungan et al. (2003) and Gan et al. (2000)]
K_{OC} ml (g OC)$^{-1}$	OC-normalized soil partition coefficient. *chloropicrin:* 66 *13D:* 28	**calibrated from field 1 data**
d (cm)	boundary layer depth (tarp permeability) *chloropicrin:* 2230 *13D:* 1326	**calibrated from field 1 data**

Figure A-1.

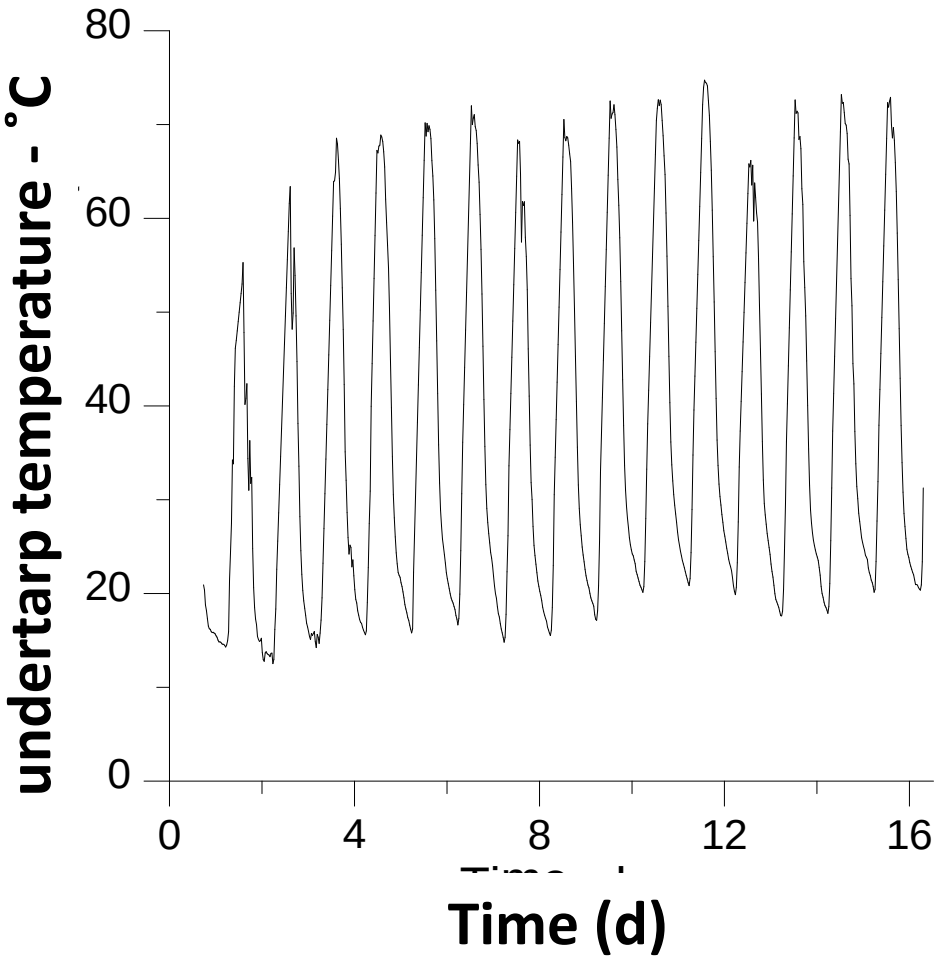

Figure A-2.

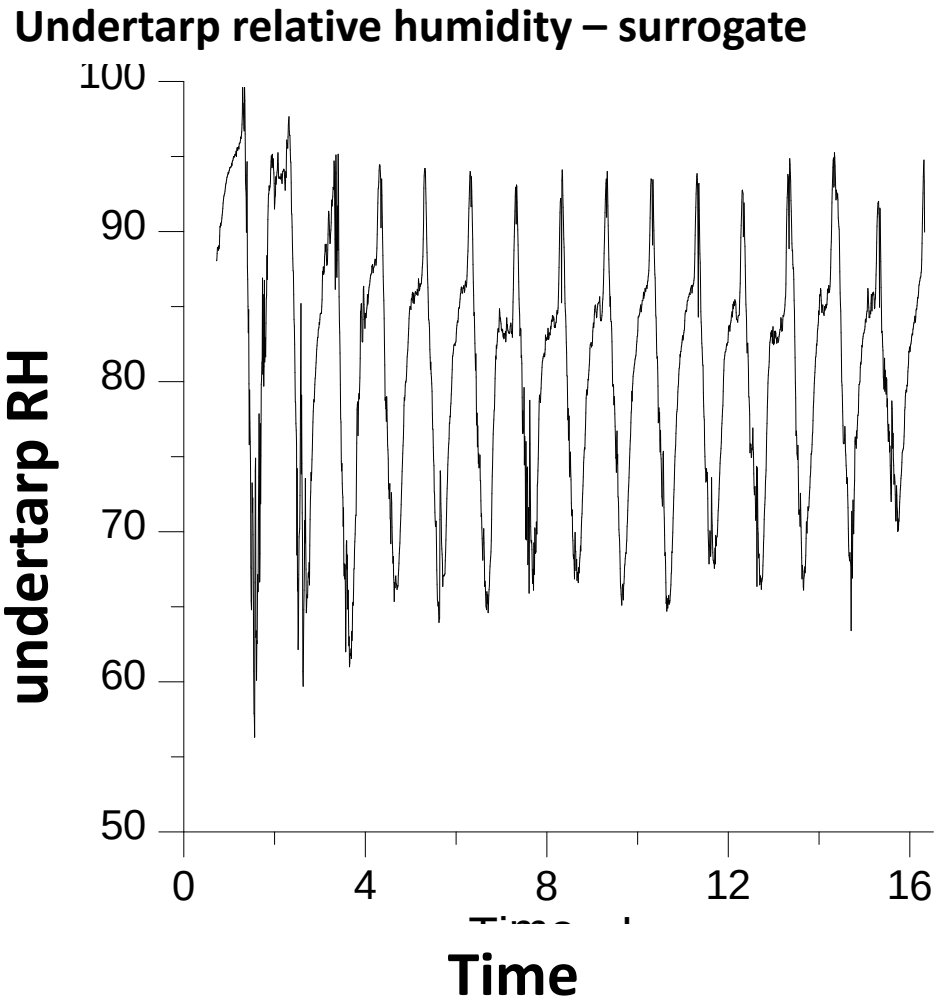
Undertarp relative humidity – surrogate
undertarp RH
100
90
80
70
60
50
0
4
8
12
16
Time

Figure A-3.

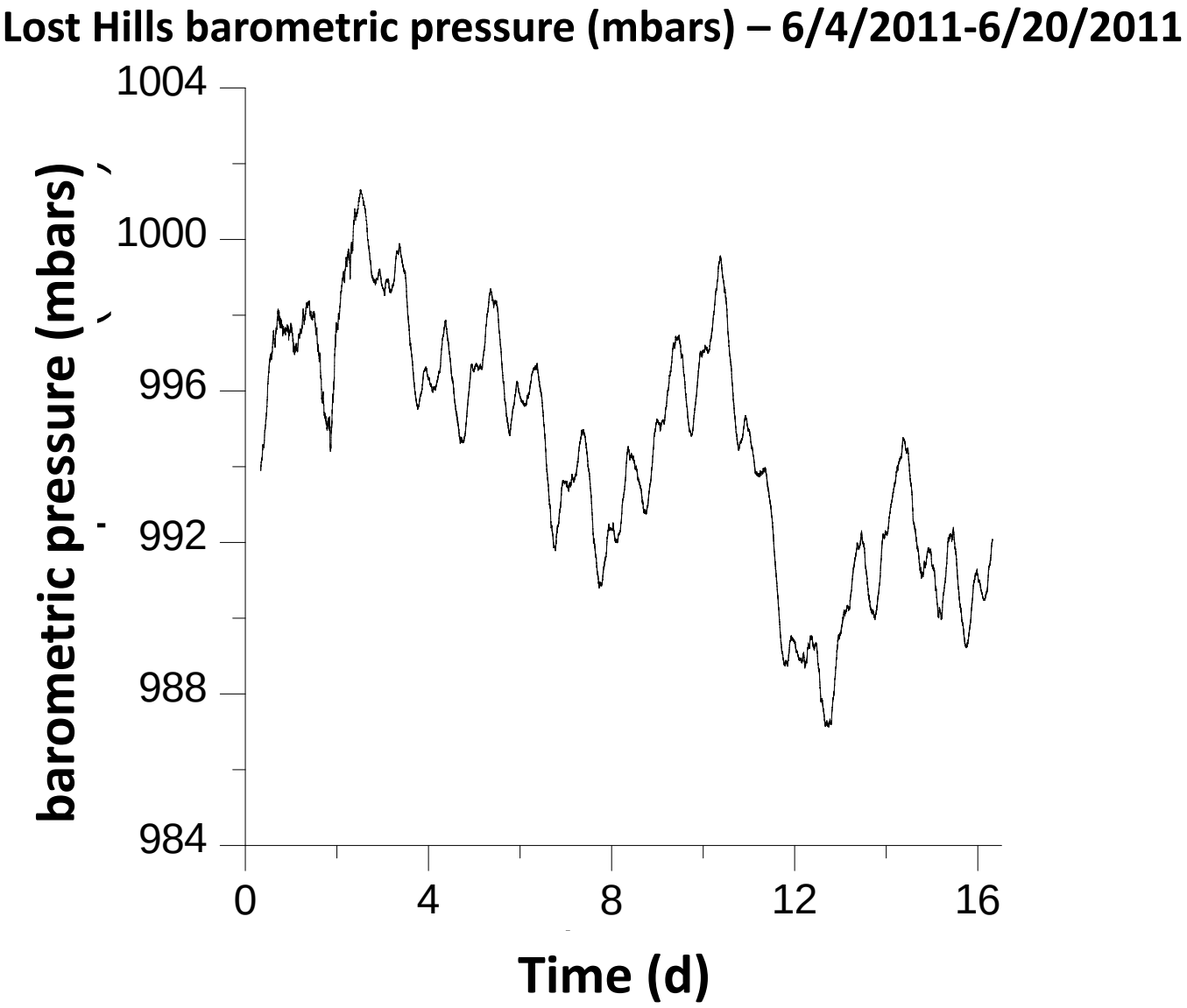
Lost Hills barometric pressure (mbars) – 6/4/2011-6/20/2011
barometric pressure (mbars)
1004
1000
996
992
988
984
0
4
8
12
16
Time (d)